LAWRENCE
LIVERMORE
NATIONAL
LABORATORY

LLNL-JRNL-412473

Erratum: "Stimulated Brillouin Backscattering and Ion Acoustic Wave Secondary Instability" [Phys. Plasmas 16, 032701 (2009)]

Bruce I. Cohen, Edward A. Williams, Richard L. Berger, Denis Pesme, Caterina Riconda

April 23, 2009

Physics of Plasmas

Disclaimer

This document was prepared as an account of work sponsored by an agency of the United States government. Neither the United States government nor Lawrence Livermore National Security, LLC, nor any of their employees makes any warranty, expressed or implied, or assumes any legal liability or responsibility for the accuracy, completeness, or usefulness of any information, apparatus, product, or process disclosed, or represents that its use would not infringe privately owned rights. Reference herein to any specific commercial product, process, or service by trade name, trademark, manufacturer, or otherwise does not necessarily constitute or imply its endorsement, recommendation, or favoring by the United States government or Lawrence Livermore National Security, LLC. The views and opinions of authors expressed herein do not necessarily state or reflect those of the United States government or Lawrence Livermore National Security, LLC, and shall not be used for advertising or product endorsement purposes.

Erratum: "Stimulated Brillouin Backscattering and Ion Acoustic Wave Secondary Instability" [Phys. Plasmas 16, 032701 (2009)]

B. I. Cohen, E. A. Williams, and R. L. Berger

Lawrence Livermore National Laboratory

P.O. Box 808, Livermore, CA 94551

D. Pesme[1] and C. Riconda[2]

[1]Centre de Physique Théorique, École Polytechnique, 91128 Palaiseau Cedex, France

[2]PAPD/LULI, Université Paris 6, CNRS, CEA, École Polytechnique, 3 rue Galilée, 94200 Ivry-sur-Seine, France

PACS: 52.38.-r 52.38.Bv

This Erratum addresses errors that occurred in some of the analysis in our recent publication (Ref. 1). The main elements of Ref. 1 are (1) the presentation of kinetic simulations of stmulated Brillouin backscattering (SBS) and the accompanying secondary instability of the primary SBS ion acoustic wave (IAW) with and without the inclusion of the second harmonic of the primary IAW; (2) analyses of the four-wave (primary IAW, low-frequency IAW, and two sidebands of the primary IAW) and seven-wave (includes the second harmonic of the primary IAW and its two sidebands, as well as the four waves defined in the foregoing) dispersion relations for the secondary IAW instability; (3) comparisons of the results of solving the dispersion relations to the two particle simulations; (4) mode coupling calculations for SBS and the four-wave system of IAWs

that model the particle simulations; and (5) a discussion and summary. However, the simplified 7-wave dispersion relation used in Ref. 1 propagated a typographical error in Eq.(44) in Ref. 2, the Pesme, Riconda, and Tikhonchuk (PRT) paper. This Erratum corrects Eq.(44) of Ref. 2 (discussed in more detail in an Erratum[3] for Ref. 2) and revises Sec. IV of Ref. 1 by correcting the analysis and comparisons of the 4-wave and 7-wave dispersion relations, and the comparison of the 7-wave dispersion relation to the particle simulations.

We find that the results of the corrected 7-wave dispersion relation are *not* profoundly different from the corresponding results in Ref. 1 and the 7-wave growth rates of the most unstable modes are more similar to the results of the 4-wave dispersion relation. The main results of Ref. 1 are unchanged: (1) the particle simulations exhibit a secondary IAW instability that is a modulational instability involving parallel and obliquely propagating IAWs; (2) the two types of particle simulation exhibit similar spectra, and the second harmonic IAW is a transient feature in the first particle simulation that is not well differentiated from the noise in the streak spectra shown in Ref. 1; (3) the 4-wave dispersion relation fits the simulation data relatively well, and only the 4-wave dispersion relation is applicable to the simulation with the second harmonic IAW suppressed; (4) the results of the 7-wave dispersion relation do not differ profoundly from the 4-wave results for the modulational instability when frequency mismatch effects are included; and (5) it is problematic justifying the application of the 7-wave dispersion relation even to the first particle simulation because the second harmonic signal is either transient or weak. The 7-wave dispersion relation is not a primary focus of Ref. 1.

In Ref. 1 a typographical error in Eq. (44) of the earlier PRT publication (Ref. 2) was repaired late in the galley-proof stage. The correction involved the term $[\bar{\varepsilon}(-1)-\frac{4\eta_{2s}|\tilde{\phi}_a|^2}{\bar{\varepsilon}(-2)}]$ on the left side of Eq. (11a) of Ref. 1, which corrected $[\bar{\varepsilon}(-1)-\frac{4\eta_{2s}|\tilde{\phi}_a|^2}{\bar{\varepsilon}(2)}]$ [containing the typographical error $\bar{\varepsilon}(2)$ instead of $\bar{\varepsilon}(-2)$] on the left side of Eq. (44) in Ref. 2, with the various quantities defined following Eq. (11a) in Ref. 1 and in Eq.(1b) here. Regrettably, Ref. 1 was posted on line before the solutions of the incorrect dispersion relation Eq.(44) of Ref. 2, appearing in Figs. 5c, 5d, 6c, 6d, 7, 8c, 8d, 9, 10c, and 10d of Ref. 1, could be re-examined. Thus, the results plotted in these figures in Ref. 1 based on the original incorrect 7-wave dispersion relation are inconsistent with Eq.(11a) in Ref. 1 and are incorrect. In addition, Pesme, Riconda, and Tikhonchuk realized after the publication of Ref. 1 that the corrected Eq.(44) does not accurately represent the H2 decay of the second harmonic decay of the primary ion acoustic wave (IAW) into a sideband and a lower-frequency IAW.[2,3] This erratum corrects the results for the seven-wave dispersion relation described in the preceding.

In the Erratum[3] for Ref. 2, Pesme, Riconda, and Tikhonchuk have presented a revised simplified dispersion relation [corresponding to the Korteweg-de-Vries (KdV) limit] for the seven-wave system of ion acoustic waves based on Eq.(39) in Ref. 2:

$$\bar{\varepsilon}^R(0)\{[\bar{\varepsilon}(1)-\frac{4\eta_{2s}|\tilde{\phi}_a|^2}{\bar{\varepsilon}(2)}][\bar{\varepsilon}(-1)-\frac{4\eta_{2s}|\tilde{\phi}_a|^2}{\bar{\varepsilon}(-2)}]-\frac{4\eta_{2m}^2|\tilde{\phi}_a|^4}{[\bar{\varepsilon}_2(0,0)]^2}\}=4\left|\tilde{\phi}_a\right|^2\{[\bar{\varepsilon}(-1)-\frac{4\eta_{2s}|\tilde{\phi}_a|^2}{\bar{\varepsilon}(-2)}](1+\eta_+)^2$$
$$+[\bar{\varepsilon}(1)-\frac{4\eta_{2s}|\tilde{\phi}_a|^2}{\bar{\varepsilon}(2)}](1+\eta_-)^2+4\left|\tilde{\phi}_a\right|^2[\frac{\eta_{2m}}{\bar{\varepsilon}_2(0,0)}](1+\eta_+)(1+\eta_-)\} \qquad (1a)$$

with

$$\bar{\varepsilon}^R(0) = \bar{\varepsilon}(0) - \frac{4\eta_{2m}^2\eta_{2s}|\tilde{\phi}_a|^4}{[\bar{\varepsilon}_2(0,0)]^2}[\frac{1}{\bar{\varepsilon}(2)} + \frac{1}{\bar{\varepsilon}(-2)}]$$

$$\bar{\varepsilon}_2(0,0) = 3k_a^2(1+\delta\Omega_{mis}), \quad \delta\Omega_{mis} = \frac{2}{3}\frac{\delta\omega_{mis}}{\omega^3(k_a)}, \quad \delta\omega_{mis} = \omega_a - k_a/(1+k_a^2)$$

$$\bar{\varepsilon}(0) = 1 + k^2 - k^2/\omega^2, \ \bar{\varepsilon}(\pm 1) = 1 + k_\pm^2 - k_\pm^2/\omega_\pm^2, \quad \bar{\varepsilon}(\pm 2) = 1 + k_{2\pm}^2 - k_{2\pm}^2/\omega_{2\pm}^2 \qquad (1b)$$

$$k_\pm^2 = (k_x \pm k_a)^2 + k_y^2, \omega_\pm = \omega \pm \omega_a, k_{2\pm}^2 = (k_x \pm 2k_a)^2 + k_y^2, \omega_{2\pm} = \omega \pm 2\omega_a$$

$$\eta_\pm = 2\frac{\eta_{2m}\eta_{2s}|\tilde{\phi}_a|^2}{[\bar{\varepsilon}_2(0,0)]}\frac{1}{\bar{\varepsilon}(\pm 2)}$$

where η_{2s}, η_{2m} = 0 or 1, $\delta\omega_{mis} \equiv \Delta\omega_a/\omega_{pi}$, and $|\Delta n_a/n_e| = 2|\tilde{\phi}_a|$; and in Eq.(1) we use units: $\tilde{\phi}_a = e\tilde{\phi}_a/T_e, k = k\lambda_e, \omega = \omega/\omega_{pi}$ as in Ref. 2 to streamline in the notation. Equation (1a) corresponds exactly to the KdV limit of the general dispersion relation (39) in Ref. 2, *i.e.*, to the limits $V_2^{stab} = 2$ for all the second-order coupling coefficients, and $V_3^{stab} = 0$ for all the third-order coupling coefficients. Equation (44) of Ref. 2 corresponds to the approximation $\eta_+ = \eta_- = 0$, and this approximation is *a priori* incorrect for the decay H2 instability. Equation (1a) corrects Eq.(44) in Ref. 2 and Eq.(11a) in Ref. 1.

Equation (44) in Ref. 2, Eq.(11a) in Ref. 1, and Eq.(1a) yield identical results for the four-wave limit of the general dispersion relations ($\eta_{NR}, \eta_{2s}, \eta_{2m}$ = 0). Thus, all of the 4-wave results in Ref. 1 are unaffected by the correction to Eq.(44) in Ref. 2 and the revised dispersion relation in (1a) here. For the modulational instability investigated in Ref. 1 the renormalization term $-\eta_{NR}9|\tilde{\phi}_a|^2$ in $\bar{\varepsilon}^R(0)$ in Eq.(11) of Ref. 2 is unimportant so that the PRT 7nr-wave roots (η_{NR}=0) in Ref. 1 differ insignificantly from the PRT 7-wave (η_{NR}=1) results. This renormalization term has been dropped in the KdV approximation leading to Eq.(1a) here. Analysis of Eq.(1a) in Ref. 3 and careful comparison to the more general dispersion relation Eq.(39) in PRT show that Eq.(1a) yields valid results for the modulational instability only in the limit that $k_a\lambda_e$<<1. For the

case of interest in Ref. 1 where $k_a\lambda_e$=0.36, the more general dispersion relation Eq.(39) in PRT must be used.

We now compare the 4-wave and 7-wave dispersion relations for the modulational instability and revise the relevant illustrations and discussion in Ref. 1 to accommodate the corrections in the 7-wave dispersion relation. We employ the general 7-wave dispersion relation Eq.(39) in PRT in which the mode coupling coefficients V2 and V3 have been approximated by their lowest order expression as derived in Appendix B of Ref. 2. Motivated by the particle simulation results in Ref. 1, we restrict ourselves to the modulational instability, so that we exclude consideration of the three-wave decay of the second harmonic IAW. Figures 1-6 here replace Figures 5-10 in Ref. 1 and show comparisons of the solutions of four-wave and seven-wave dispersion relations corresponding to the modulational instability.

We consider $\Delta\omega_a/\omega_{al}$={-0.01, 0, and 0.01} in Figs. 1 and 2 and note the sensitivity of the secondary instability with respect to the mismatch frequency. Using a small mismatch frequency is motivated by the BZOHAR observations and by the argument on the cancellation of the net effect of the frequency shifts due to trapping in Ref. 1. We consider the solutions of the 4-wave and 7-wave dispersion relations for the secondary IAW instability in Figs. 1-6 for parameters relevant to the BZOHAR simulations. In Fig. 1 are shown contours of the growth rate as a function of $k_x\lambda_e$ and $k_y\lambda_e = k_\perp\lambda_e$ for $|\Delta n_a / n_e| = 0.12,\ k_a\lambda_e = 0.36,\ \Delta\omega_a / \omega_{al} = 0$. The peak four-wave (Ref. 4) growth rate is Im ω/ω_{al} =0.0071 (Fig. 1a), while the peak PRT four-wave growth rate is 0.0051 (Fig. 1b); and the locations of the roots are indicated on the plots near the half-harmonic in $k_x\lambda_e$ but with substantial values of $k_y\lambda_e$. The peak instability growth rate for the 7-wave

dispersion relation in Figs. 5c is 0.0060 occurring near the half-harmonic in k_x and at slightly smaller k_y than in the 4-wave dispersion relation, and the structure of the roots differs. The growth rate for the secondary instability observed in the first BZOHAR simulation shown in Fig. 2c of Ref. 1 is Im ω/ω_{al}~0.0073 for $\Delta n_a/n_e$~0.12, and Im ω/ω_{al}~0.013 in the second simulation shown in Fig. 3c in Ref. 1 for the higher IAW amplitude $\Delta n_a/n_e$~0.18 (for this amplitude and $\Delta\omega_a$=0, the PRT 4-wave peak growth rate is Im ω/ω_{al}~0.01).

The roots shown in Fig. 1 correspond to modulational instability: $|\bar{\varepsilon}(\pm 1)| \sim O(10^{-2}) << |\bar{\varepsilon}(\pm 2)|, |\bar{\varepsilon}(0)| \sim O(1)$. Instability in the 7-wave case extends to $k_y\lambda_e$=0 and a finite value of $k_x\lambda_e$ smaller than the half-harmonic of the primary IAW for $\Delta\omega_a$=0. The modulational instability with k_y=0 will be referred to as a "1D modulational instability" and does not exist in the limit of the 4-wave dispersion relation for $\Delta\omega_a$=0. The most unstable, obliquely propagating mode can be approximated, in the limit $|\Delta n_a / n_e| << 1$ and $k_a\lambda_e$ <<1 by $k_y / k_x \approx \sqrt{3}\, k_a \lambda_e$ (see Eq.(80) and Sec. VI.B.2 of Ref. 2). The modulational instability appears to play an important role in the interpretation of the BZOHAR results. References 2 and 3 discuss the other branches of instability (three-wave decay of the primary IAW, the three-wave decay of the second harmonic, and hybrids of the branches of instability) supported by Eq.(39) of Ref. 2 in some detail.

Does the second harmonic decay occur in the first of the BZOHAR simulation examples in Ref. 1? The wave number spectrum of the IAWs observed in the BZOHAR simulations shows no signature of modes with very small values of k_x and $k_y\lambda_e$=O(0.1), which could indicate that there is no instability corresponding to the decay of the second harmonic of the primary IAW. On the other hand, this domain of very small values of k_x

and $k_y\lambda_e=O(0.1)$ is not the only signature of the influence of the second harmonic. Indeed, there are at least two other signatures of the influence of the second harmonic: (i) the "1D modulational instability" domain exists in the case of the seven-wave dispersion relation for $\Delta\omega_a=0$, as observed when comparing Fig. 1a or Fig. 1b (4-wave) with Fig. 1c (7-wave); (ii) the "2D modulational instability" domain corresponding to the domain $k_x \sim k_a/2$ and $k_y / k_x \approx \sqrt{3}\, k_a \lambda_e$ also involves a contribution from the second harmonic, as can be checked by comparing Fig. 1(b) (4 wave) with Fig. 1c (7 wave) for $\Delta\omega_a=0$, Fig. 2a (4 wave) with Fig. 2c (7 wave) $\Delta\omega_a<0$, and Fig. 2b (4 wave) with Fig. 2d (7 wave) for $\Delta\omega_a>0$. The reason why the second harmonic may significantly modify the modulational instability in the "2D modulational instability" domain can be explained as follows: the decay product frequencies and wave numbers of the second harmonic decay are ($\sim 5/2\ \omega_a$, $\sim 5/2\ k_a$) for the upper component and ($\sim 3/2\ \omega_a$, $\sim 3/2\ k_a$) for the lower one. Thus, this lower component is able to interact with the upper component of the modulational instability. Therefore, the modulational instability and the second harmonic decay instability may coalesce and give rise to a hybrid root in the vicinity of the intersection of the resonant curves of the modulational instability and of the secondary decay instability. This domain corresponds to the "2D modulational instability". However, these two different structures of the modulational root observed in Fig. 1c and resulting from the 7-wave dispersion relation are not exclusive features of the 7–wave dispersion relation. Indeed, Fig. 2a, corresponding to the parameters $|\Delta n_a / n_e| = 0.12,\ k_a\lambda_e = 0.36,\ \Delta\omega_a / \omega_{al} = -0.01$, displays a structure for the root of the PRT 4-wave dispersion relation, which is very similar to the structure observed in Fig. 1c for the PRT 7-wave dispersion relation: unstable IAWs near the primary IAW's half-

harmonic in $k_x\lambda_e$ with substantial values of $k_y\lambda_e$, namely $k_y\lambda_e \approx \sqrt{3}\,(k_a\lambda_e)k_x\lambda_e$, (the "2D modulational instability"), and unstable modes extending to smaller $k_x\lambda_e$ and $k_y\lambda_e$=0 (the "1D modulational instability" domain).

The "2D modulational instability" structure is a good match to the BZOHAR 2D wave number spectra shown in Fig. 4 of Ref. 1. However, there are also 1D modes present in the spectra, and the electrostatic wave spectra for the *one-dimensional* SBS simulations shown in Fig. 4 of Ref. 12 exhibit a spread of longer wavelength IAWs accompanying the instability of the SBS IAW. Thus, it is significant that the modulational instability can have unstable modes with $k_y\lambda_e$=0, in addition to the unstable modes with finite $k_y\lambda_e$. Both 4-wave and 7-wave dispersion relations support 1D and 2D modulational instability depending on the values of $\Delta\omega_a$ used. We also note that the structure of the roots in Fig. 2 shows a significant asymmetry with respect to the sign of the mismatch frequency $\Delta\omega_a$ (Figs. 2a and 2c vs. Figs. 2b and 2d). This asymmetry is more pronounced at larger values of $|\Delta\omega_a|$ and is addressed in Ref. 2. All of the unstable roots plotted in Figs. 1and 2 are modulational modes as confirmed by evaluating the dielectric functions of the unstable product waves.

In Fig. 3 we show a scan of the most unstable growth rate for modulational instability as a function of $|\Delta n_a / n_e|$ for $k_a\lambda_e = 0.36$, $\Delta\omega_a / \omega_{al} = 0$. The PRT 7-wave and 4-wave roots have growth rates scaling as $|\Delta n_a / n_e|^2$ for small wave amplitudes. The 4-wave roots have slightly weaker growth rates. A consequence of the quadratic scaling of the growth rates with IAW amplitude is that the secondary instability temporal behavior will be sensitive to the time dependence of the SBS IAW amplitude. The dependence of the modulational instability roots on $|\Delta n_a / n_e|$ is further elaborated in Fig.

4 where the growth rates, frequencies, and wave numbers of the fastest growing modes are plotted as functions of $|\Delta n_a / n_e|$. The structures of the solutions from the PRT 4-wave and 7-wave dispersion relations are generally similar, but there are quantitative differences. The increased growth rate accompanying the larger IAW amplitude in the second BZOHAR example in Sec. II of Ref. 1 follows from the scaling of the growth rates with $|\Delta n_a / n_e|^2$.

In Figs. 5 and 6 we show solutions for the growth rates, frequencies, and wave numbers of the most unstable modulational modes as functions of the mismatch frequency $\Delta\omega_a$ with $|\Delta n_a / n_e| = 0.12$, $k_a \lambda_e = 0.36$ for the 4-wave dispersion relation of Ref. 4 and the PRT 4-wave and 7-wave dispersion relations. The structure of the roots is generally similar, but quantitative differences are evident. We note that the smallest growth rates for the four-wave dispersion relations occur at $\Delta\omega_a$=0, while the smallest growth rates are shifted to $\Delta\omega_a/\omega_{a1} \sim -0.02$ for the seven-wave dispersion relations. The results in Fig. 5 provide some insight into why the maximum growth rates in Figs. 1, 2, and 3 for the 4-wave dispersion relations are either smaller or larger than for the 7-wave dispersion relations. The dependence of the modulational instability roots on the frequency mismatch is important, and faster growth rates are observed for sufficiently large $|\Delta\omega_a|$ than for $\Delta\omega_a$=0.

For small values of $|\Delta\omega_a/\omega_{a1}|$ the solutions of the dispersion relations yield $\mathrm{Re}\,\omega/\omega_{a1}$~0.3-0.4 which sets the separation of the unstable sidebands of the primary IAW and compares favorably to the observed frequency spectra in Figs. 2b and 3b of Ref. 1. For the range of mismatch frequencies considered, there is no instability of the IAW corresponding to a resonant three-wave decay of the primary SBS IAW. The BZOHAR

power spectra in Figs. 2b and 3b in Ref. 1 suggest that the SBS IAW experiences a small negative frequency shift at a time preceding the onset of the secondary instability. However, if the instability products share the same proportional frequency shift due to trapping, then the net frequency shift might cancel.[1] In addition, if ion trapping is affecting all of the IAW instability products (the ion trapping width as a fraction of the IAW phase velocity $v_{tr}/c_s \sim |\Delta n_a/n_e|^{1/2} \sim 0.3$ is relatively large in the BZOHAR examples), then the ion Landau damping of all of the instability product waves will be reduced, which reduces thresholds and increases the net growth rates for the secondary instability relative to the case with finite damping of the instability products. We note that the growth rates for the modulational instability become too large compared to the BZOHAR observations in Figs. 1, 2, and 3 of Ref. 1 if $|\Delta\omega_a|$ is too large. It seems that the best agreement with the BZOHAR observations is obtained for $\Delta\omega_a/\omega_a=0$ or -0.01 with the caveat that IAW damping has not been included in the analysis of the dispersion relations.

We cannot assert with absolute certainty that the second harmonic IAW has no influence on the secondary instability observed in the first BZOHAR simulation described in Sec. II of Ref. 1. However, the analysis of the secondary instability presented here and in Ref. 1 suggests that the 4-wave dispersion relation can yield growth rates and spectra similar to the simulation results of both particle simulations in Ref. 1 for reasonable parameters. The results of the analysis of the 4-wave and 7-wave dispersion relations indicate that the modulational instability is a good candidate to explain the simulation observations and that coupling to the second harmonic of the SBS IAW is *not* a required element in the secondary IAW instability seen in the particle simulations. The

conclusions derived from the solutions of the general 7-wave dispersion relation, Eq.(39) of PRT, for modulational instability support the main findings of Ref. 1.

This work was performed under the auspices of the Department of Energy/NNSA by the Lawrence Livermore National Laboratory (LLNL) under Contract No. DE-AC52-07NA27344. This work was partially funded by the Laboratory Directed Research and Development Program at LLNL under project tracking code 08-ERD-031. Two of the authors (DP and CR) would like to acknowledge the support of the French Agence Nationale de la Recherche, Project No ANR-07-BLAN-0004 "CORPARIN".

References

[1] B. I. Cohen, E. A. Williams, R. L. Berger, D. Pesme, and C. Riconda, Phys. Plasmas **16**, 032701 (2009).

[2] D. Pesme, C. Riconda, and V. Tikhonchuk, Phys. Plasmas **12**, 092101 (2005).

[3] D. Pesme, C. Riconda, and V. Tikhonchuk, "Erratum: Parametric instability of a driven ion-acoustic wave [D. Pesme, C. Riconda, and V. Tikhonchuk, Phys. Plasmas **12**, 092101 (2005)], submitted to Phys. Plasmas.

[4] B. I. Cohen, B. F. Lasinski, A. B. Langdon, E. A. Williams, Phys. Plasmas **4**, 956 (1997).

Figure Captions

Figure 1. (Color online) Solutions of the (a) 4-wave dispersion relation (Ref. 4), (b) PRT 4-wave dispersion relation, and (c) 7-wave dispersion relation Eq.(39) in PRT including V3 terms and using App. B in Ref. 2 for the coupling coefficients, for modulational instability growth rates $\mathrm{Im}\omega/\omega_{al}$ vs. $k_y\lambda_e$ and $k_x\lambda_e$, with $k_a\lambda_e$=0.36, $|\Delta n_a/n_e|$=0.12, $\Delta\omega_a$=0, and cold ions.

Figure 2. (Color online) Solution of the (a),(b) PRT 4-wave and (c), (d) 7-wave dispersion relation Eq.(39) as in Fig. 1 for modulational instability growth rates $\mathrm{Im}\omega/\omega_{al}$ vs. $k_y\lambda_e$ and $k_x\lambda_e$, with $k_a\lambda_e$=0.36, $|\Delta n_a/n_e|$=0.12 and cold ions with (a), (c) $\Delta\omega_a/\omega_{al}$ =-0.01 and (b), (d) $\Delta\omega_a/\omega_{al}$ =0.01

Figure 3. (Color online) Solutions of the PRT four-wave and seven-wave dispersion relations for modulational instability growth rates $\mathrm{Im}\omega/\omega_{al}$ vs. $|\Delta n_a/n_e|$ for the most unstable mode, with $k_a\lambda_e$=0.36, $\Delta\omega_a$=0 and cold ions.

Figure 4. (Color online) Solutions of the dispersion relations for modulational instability growth rates $\mathrm{Im}\omega/\omega_{al}$, $\mathrm{Re}\omega/\omega_{al}$, $k_y\lambda_e$, and $k_x\lambda_e$ vs. $|\Delta n_a/n_e|$ for the most unstable mode, with $k_a\lambda_e$=0.36, $\Delta\omega_a$=0, and cold ions: (a) PRT 4-wave dispersion relation and (b) PRT 7-wave dispersion relation.

Figure 5. (Color online) Solutions of the 4-wave (Ref. 4), PRT 4-wave and 7-wave dispersion relations for modulational instability growth rates $\mathrm{Im}\omega/\omega_{al}$ vs. $\Delta\omega_a/\omega_{al}$ for the most unstable mode, with $k_a\lambda_e$=0.36, $|\Delta n_a/n_e|$=0.12, and cold ions.

Figure 6. (Color online) Solutions of the dispersion relations for modulational instability growth rates $\mathrm{Im}\omega/\omega_a$, $\mathrm{Re}\omega/\omega_{al}$, $k_y\lambda_e$, and $k_x\lambda_e$ vs. $\Delta\omega_a/\omega_{al}$ for the most unstable mode, with

$k_a\lambda_e$=0.36, $|\Delta n_a/n_e|$ =0.12, and cold ions: (a) 4-wave dispersion relation from Ref. 4, (b) PRT 4-wave dispersion relation, and (c) PRT 7-wave dispersion relation.

Figure 1

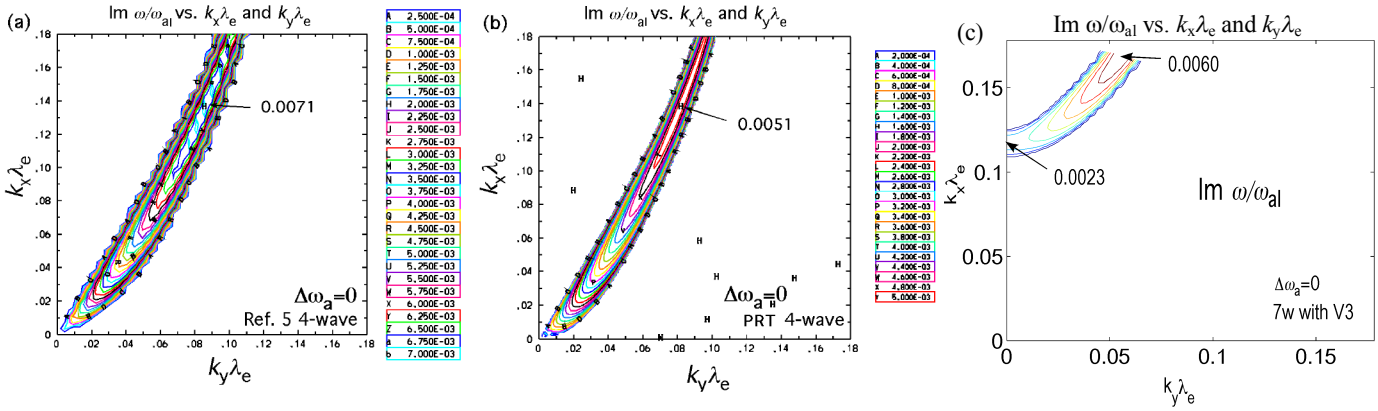
(a)
Im ω/ω_al vs. k_xλ_e and k_yλ_e
0.0071
Δω_a=0
Ref. 5 4-wave
k_xλ_e
k_yλ_e
(b)
Im ω/ω_al vs. k_xλ_e and k_yλ_e
0.0051
Δω_a=0
PRT 4-wave
k_xλ_e
k_yλ_e
(c)
Im ω/ω_al vs. k_xλ_e and k_yλ_e
0.0060
0.0023
Im ω/ω_al
Δω_a=0
7w with V3
k_xλ_e
k_yλ_e

Figure 2

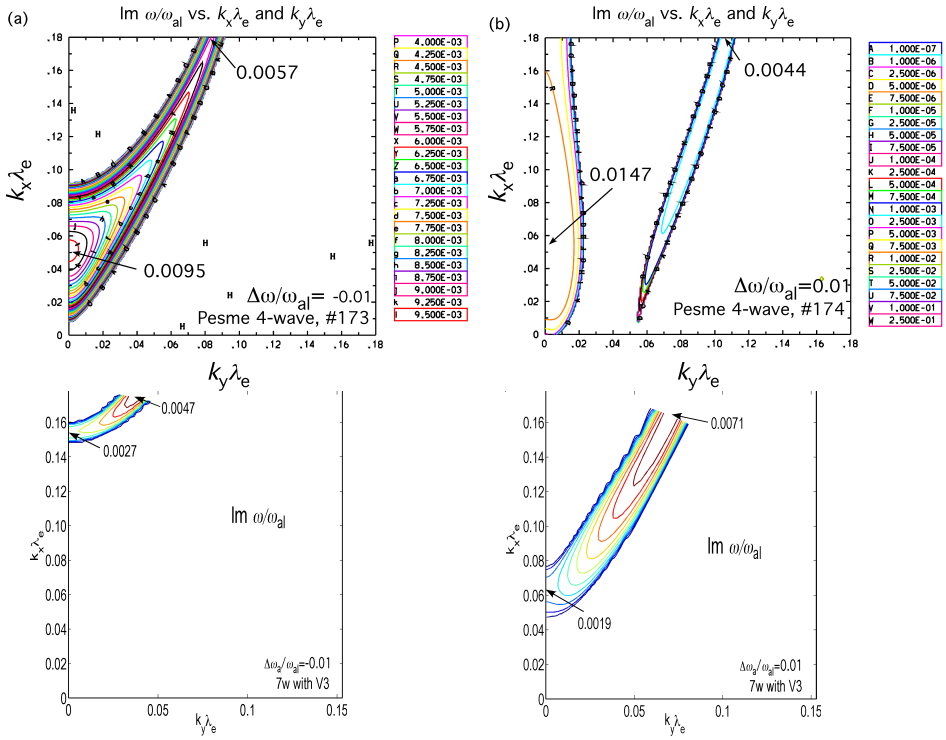
(a)
Im ω/ω_al vs. k_xλ_e and k_yλ_e
0.0057
0.0095
Δω/ω_al= -0.01
Pesme 4-wave, #173
P 4.000E-03
Q 4.250E-03
R 4.500E-03
S 4.750E-03
T 5.000E-03
U 5.250E-03
V 5.500E-03
W 5.750E-03
X 6.000E-03
Y 6.250E-03
Z 6.500E-03
a 6.750E-03
b 7.000E-03
c 7.250E-03
d 7.500E-03
e 7.750E-03
f 8.000E-03
g 8.250E-03
h 8.500E-03
i 8.750E-03
j 9.000E-03
k 9.250E-03
l 9.500E-03
(b)
Im ω/ω_al vs. k_xλ_e and k_yλ_e
0.0044
0.0147
Δω/ω_al=0.01
Pesme 4-wave, #174
A 1.000E-07
B 1.000E-06
C 2.500E-06
D 5.000E-06
E 7.500E-06
F 1.000E-05
G 2.500E-05
H 5.000E-05
I 7.500E-05
J 1.000E-04
K 2.500E-04
L 5.000E-04
M 7.500E-04
N 1.000E-03
O 2.500E-03
P 5.000E-03
Q 7.500E-03
R 1.000E-02
S 2.500E-02
T 5.000E-02
U 7.500E-02
V 1.000E-01
W 2.500E-01
k_yλ_e
k_xλ_e
0.0047
0.0027
Im ω/ω_al
Δω_2/ω_al=-0.01
7w with V3
0.0071
0.0019
Δω_2/ω_al=0.01
7w with V3

Figure 3

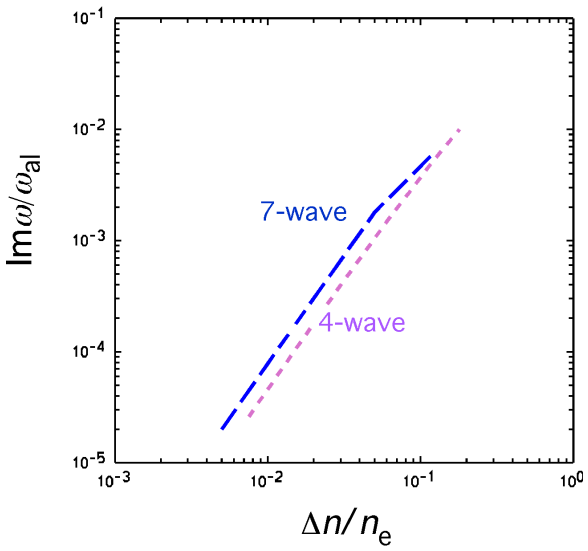
10^{-1}
10^{-2}
10^{-3}
10^{-4}
10^{-5}
$\mathrm{Im}\omega/\omega_{\mathrm{al}}$
7-wave
4-wave
10^{-3}
10^{-2}
10^{-1}
10^{0}
$\Delta n/n_{\mathrm{e}}$

Figure 4

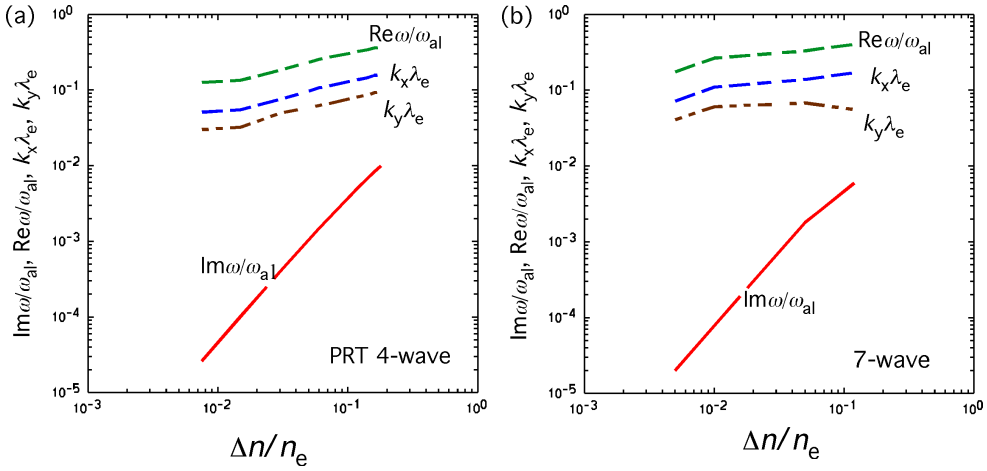
(a)
(b)
Reω/ω_{al}
$k_x\lambda_e$
$k_y\lambda_e$
Imω/ω_{al}
PRT 4-wave
7-wave
Imω/ω_{al}, Reω/ω_{al}, $k_x\lambda_e$, $k_y\lambda_e$
$\Delta n/n_e$

Figure 5

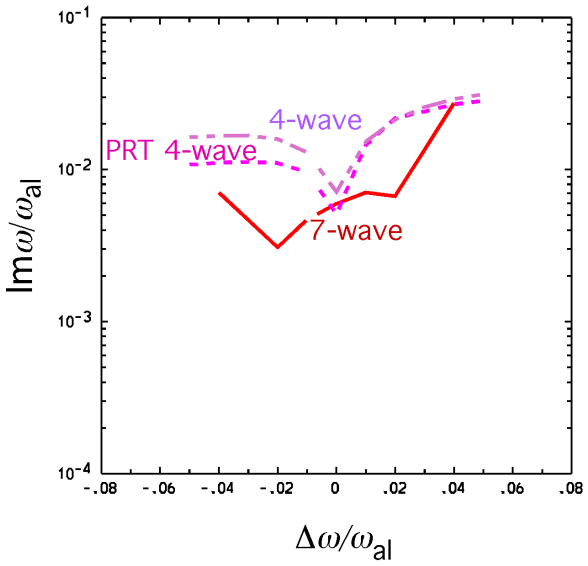
4-wave
PRT 4-wave
7-wave
Imω/ω_{al}
$\Delta\omega/\omega_{al}$
10^{-1}
10^{-2}
10^{-3}
10^{-4}
-.08
-.06
-.04
-.02
0
.02
.04
.06
.08

Figure 6

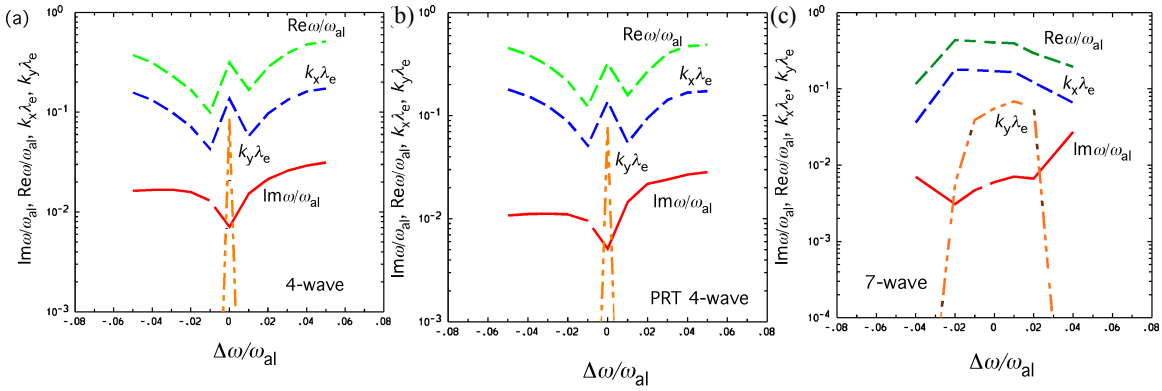
(a)
Reω/ω_al
k_xλ_e
k_yλ_e
Imω/ω_al
4-wave
Imω/ω_al, Reω/ω_al, k_xλ_e, k_yλ_e
Δω/ω_al
(b)
Reω/ω_al
k_xλ_e
k_yλ_e
Imω/ω_al
PRT 4-wave
Imω/ω_al, Reω/ω_al, k_xλ_e, k_yλ_e
Δω/ω_al
(c)
Reω/ω_al
k_xλ_e
k_yλ_e
Imω/ω_al
7-wave
Imω/ω_al, Reω/ω_al, k_xλ_e, k_yλ_e
Δω/ω_al